Aggregation-induced emission biomaterials for anti-pathogen medical applications: detecting, imaging and killing

Zicong Zhang[1], Ziwei Deng[1], Lixun Zhu[1], Jialin Zeng[1], Xu-Min Cai[2], Zijie Qiu[1], Zheng Zhao[1,3,*], Ben Zhong Tang[1,4,*]

[1] *Clinical Translational Research Center of Aggregation-Induced Emission, The Second Affiliated Hospital, School of Medicine; School of Science and Engineering; Shenzhen Key Laboratory of Functional Aggregate Materials, The Chinese University of Hong Kong, Shenzhen, Guangdong, 518172, China*

[2] *Jiangsu Co-Innovation Center of Efficient Processing and Utilization of Forest Rescources, International Innovation Center for Forest Chemicals and Materials, College of Chemical Engineering, Nanjing Forestry University, Nanjing 210037, China.*

[3] *HKUST-Shenzhen Research Institute, South Area Hi-Tech Park, Nanshan, Shenzhen, Guangdong Province, 518057, China*

[4] *Department of Chemistry, Hong Kong Branch of Chinese National Engineering Research Center for Tissue Restoration and Reconstruction, The Hong Kong University of Science and Technology, Clear Water Bay, Kowloon, Hong Kong, China*

[*] Corresponding address. E-mail addresses: zhaozheng@cuhk.edu.cn; tangbenz@cuhk.edu.cn

Key words: Aggregation-induced emission, fluorescence imaging, pathogen differentiation, pathogen inactivation

Abstract

Microbial pathogens, including bacteria, fungi, and viruses, greatly threaten the global public health. For pathogen infections, early diagnosis and precise treatment are essential to cut the

mortality rate. The emergence of aggregation-induced emission (AIE) biomaterials provides an effective and promising tool for the theranostics of pathogen infections. In this review, the recent advances about AIE biomaterials for anti-pathogen theranostics are summarized. With the excellent sensitivity and photostability, AIE biomaterials have been widely applied for precise diagnosis of pathogens. Besides, different types of anti-pathogen methods based on AIE biomaterials will be presented in detail, including chemotherapy and phototherapy. Finally, the existing deficiencies and future development of AIE biomaterials for anti-pathogen applications will be discussed.

1. Introduction

Human society has been plagued by infectious diseases at different stages of development [1]. It could be said that the history of human development is an epic against infectious diseases. Most infectious diseases are caused by pathogenic microbes, including bacterium, fungus and virus. In the 14th century, the Black Death caused by *Yersinia pestis*, raged for three centuries across the continent of Europe, killing more than 25 million people [2]. Since 2019, the COVID-19 pandemic caused by severe acute respiratory syndrome coronavirus 2 (SARS-CoV-2) has spread rapidly worldwide, infected nearly 700 million people and caused almost 7 million death [3]. Although medical level and epidemic prevention measures have been substantially improved, infectious disease is still a great threat to human health.

For pathogen infections, early diagnosis and precise treatment are essential to cut the mortality rate. At present, different technologies or methods have been developed for either fundamental research of pathogen or clinical diagnosis of pathogenic microbes, including Gram staining methods, electron microscopy (SEM, TEM, Cryo-EM), and microcolony method [4-6]. However, these techniques generally depend on expensive instruments, which also suffer the drawbacks of complicated operation, high cost, and labor-intensive and time-consuming process. On the other hand, clinical treatment aims to effectively elimination of pathogens after diagnosis. Unfortunately, due to the abuse of anti-pathogen drugs (especially antibiotics), the drug-resistant pathogenic infection has become a serious global public health issue [7, 8].

With the advantages of high sensitivity and easy operation, fluorescence technology has been widely applied in biological detection and imaging [9]. However, traditional fluorescent dyes mostly

suffer the influence of aggregation caused quenching (ACQ) effect, which limited their applications and sometimes may even cause the false negative signals in detection or diagnosis [10]. In terms of these, aggregation-induced emission (AIE) luminogens provide an excellent solution for the problems caused by ACQ materials [11]. AIE luminogens (AIEgens) indicate those luminescent materials with dim emission in solution state but enhanced emission after aggregation, the unique aggregation caused turn-on emission and enhanced photostability as well as other photoactivities (e.g. ROS: reactive oxygen species) in aggregate state make them particularly applicable for biological applications [12, 13]. After 20 years development, the application scopes of AIE materials in biological area currently have been extended to pathogens and mammalian cells related detection, tracing, therapy, and theranostics, etc [14-17]. In this review, we will summarize the recent research progress of AIE biomaterials for anti-pathogen medical theranostic applications. Firstly, the working mechanism of AIEgens-based theranostics will be briefly described. Then, the applications of AIEgens for precise diagnosis of pathogens will be discussed and some representative examples will be highlighted. In addition, different types of anti-pathogen therapeutic approaches will be presented, including chemotherapy and phototherapy. At last, the existing deficiencies and future prospective of AIE biomaterials for anti-pathogen applications will be proposed.

2. The overview of AIE

The concept of AIE was first coined by Prof. Tang in 2001, describing a photophysical phenomenon in which molecular aggregates exhibit stronger emission than the single molecules [11]. So far, the working mechanism of AIE has been well investigated, which is summarized as restriction of intramolecular motion (RIM), including restriction of intramolecular rotations (RIR) and restriction of intramolecular vibration (RIV) (Fig. 1) [13, 18]. The propeller-shaped (tetraphenylethene, TPE) or butterfly-shaped (cyclooctatetrathiophene) molecules display almost no emission in dilute solutions or single molecular state, while show intensive emission in aggregate state [19, 20]. In comparison with inorganic luminescent materials and traditional ACQ luminogens, AIEgens hold many advantages, including easy-tunable chemical structure, large Stokes shift, high sensitivity in biological microenvironments, superior photostability, good biocompatibility, excellent long-term tracking capability, and so on [21-24]. Thus, the fluorescent materials with AIE

characteristics are excellent candidates for biological imaging and diagnostic applications [15, 25].
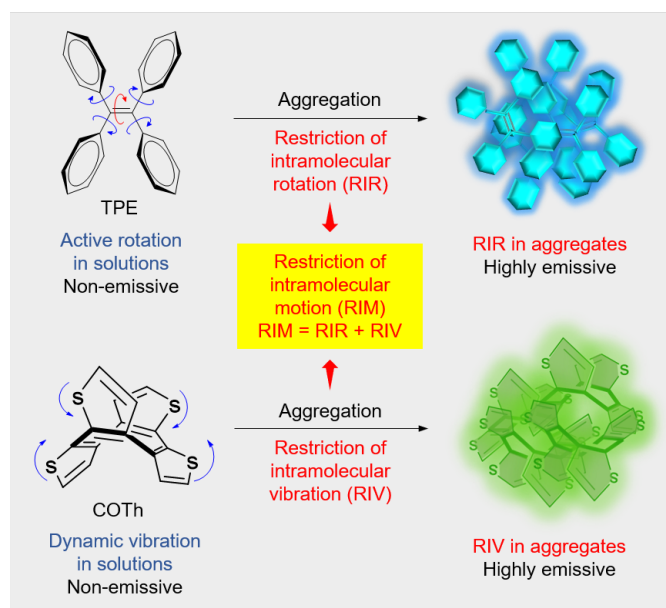

Figure 1. The phenomena of aggregation-induced emission (AIE) observed in organic molecules and the mechanisms. Tetraphenylethene (TPE) is non-emissive in tetrahydrofuran (THF) solution, while it becomes highly emissive in aggregates due to the restriction of intramolecular rotations (RIR). Cyclooctatetrathiophene (COTh) exhibited similar AIE property, which is caused by the restriction of intramolecular vibration (RIV).

Apart from the superior luminescent performance in aggregate state, AIE materials also exhibit promising photodynamic and photothermal activity through regulating the intersystem crossing efficiency and excited state molecular motion in aggregate state. The excellent photodynamic and photothermal properties of AIEgens enable their promising applications for theranostics of pathogenic infections [26-28]. The detailed working mechanism of AIE photosensitizers and photothermal agents could be principally understood by the classical Jablonski diagram as shown in Fig. 2 [29]. After excitation from the ground state (S_0) to higher excited states (S_n), the exciton will decay to the lowest singlet excited state (S_1) according to Kasha's rule, [30]. In general, there are three decay pathways for the excitons. For example, returning to S_0 state and emitting fluorescence by a radiative pathway, which potentially could be used for fluorescence sensing and imaging [31, 32]. Additionally, the S_1 can also be deactivated through nonradiative decay pathway accompanied by generating heat, which provides an pathway to develop organic photothermal agent for photothermal therapy (PTT) [33]. Besides, the excitons at S_1 can also relax to the lowest triplet state (T_1) through the intersystem crossing (ISC) to sensitize $^3O_2$ to generate reactive oxygen species

(ROS) for photodynamic therapy (PDT) [34]. Since ACQ effect will quench the singlet excited state, the ROS efficiency of ACQ photosensitizers (PSs) thus are strongly suppressed in the aggregate state [35]. As a contrast, the ROS efficiency of AIE PSs don't suffer the ACQ effect but exhibit an enhancement upon aggregation due to the suppression of non-radiative decay [15, 36].
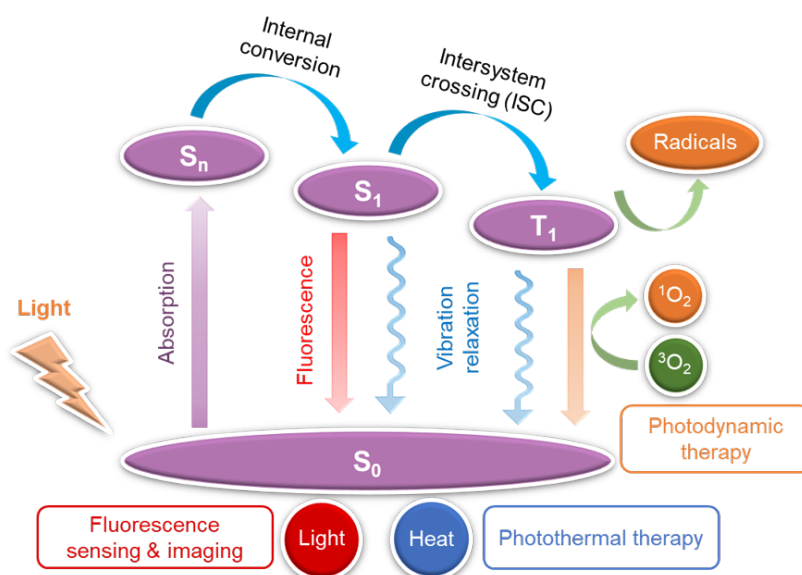

Figure 2. Working mechanism of photosensitizers and photothermal agents described by the Jablonski diagram, where S and T represent the singlet and triplet states, respectively.

3. AIE biomaterials for diagnosis of pathogens

3.1 AIE biomaterials for differentiation of bacteria

Various bacteria exist in nature [37]. In general, bacteria can be divided into two groups by Gram staining, which is a common technique used to differentiate from their cell wall constituents [4]. Compared with Gram staining, fluorescence imaging is considered to be more sensitive and convenient for detection and differentiation [9]. To date, AIE biomaterials have been widely utilized for bacterial imaging based on strategies summarized as follows. The most universal strategy is to introduce positive charges into AIE biomaterials to bind the bacterial envelope through electrostatic interaction [38], since the lipopolysaccharides (LPS), teichoic acid and peptidoglycan in the bacterial cell wall were all reported to be negatively charged [39, 40]. Michelle et al. designed an AIE probe of TTVP with two positive charges (Fig. 3A) [41]. TTVP could selectively target Gram-

positive bacteria *S. aureus* through a washing-free procedure with only 3 s of incubation period, implying its ultrafast bacterial discrimination feature. Furthermore, a receptor-targeting labeling strategy is introduced since various receptors exist on the bacterial envelope [42, 43]. Wang et al. developed a receptor-targeting AIE PS (CE-TPA) by conjugating cephalothin (a β-lactam antibiotic) with a cationic AIE probe and the probe could target penicillin-binding proteins (PBPs), which is the main target of β-lactam antibiotics (Fig. 3B) [44]. As a result, CE-TPA could target Gram-positive methicillin-resistant *Staphylococcus aureus* (MRSA). However, the probe failed to stain ampicillin-resistant *Escherichia coli* (Amp^r *E. coli*) due to the denser cell wall of Gram-negative bacteria. To achieve more stable and durable labeling, covalent labeling strategies like clickable and metabolic strategies have been developed in recent years [45, 46]. An AIE probe modified with isothiocyanate (NCS), CDPP-NCS, was utilized for covalent labeling through click reaction between NCS groups and amino groups (Fig. 3C) [47]. It is notable that the probe could stably retain on the envelope for over 48 h without leakage, enabling the monitoring of interaction between bacterium and macrophage, which benefits the study the infection process. In addition, metabolic strategies can be applied as well. [48]. D-alanine (D-Ala) could be selectively utilized by bacteria for its significant role in the synthesis of peptidoglycan. A bacteria-metabolizable AIE probe TPEPy-D-Ala that consists of D-alanine and AIE fluorophore was thus developed for fluorescence turn-on imaging of intracellular bacteria in living host cells (Fig. 3D). Notably, the septal planes of bacteria showed stronger signals owing to the ongoing peptidoglycan synthesis (the white arrows in Fig. 3D). Established on the above strategies, AIE probes have been widely applied for bacterial imaging.
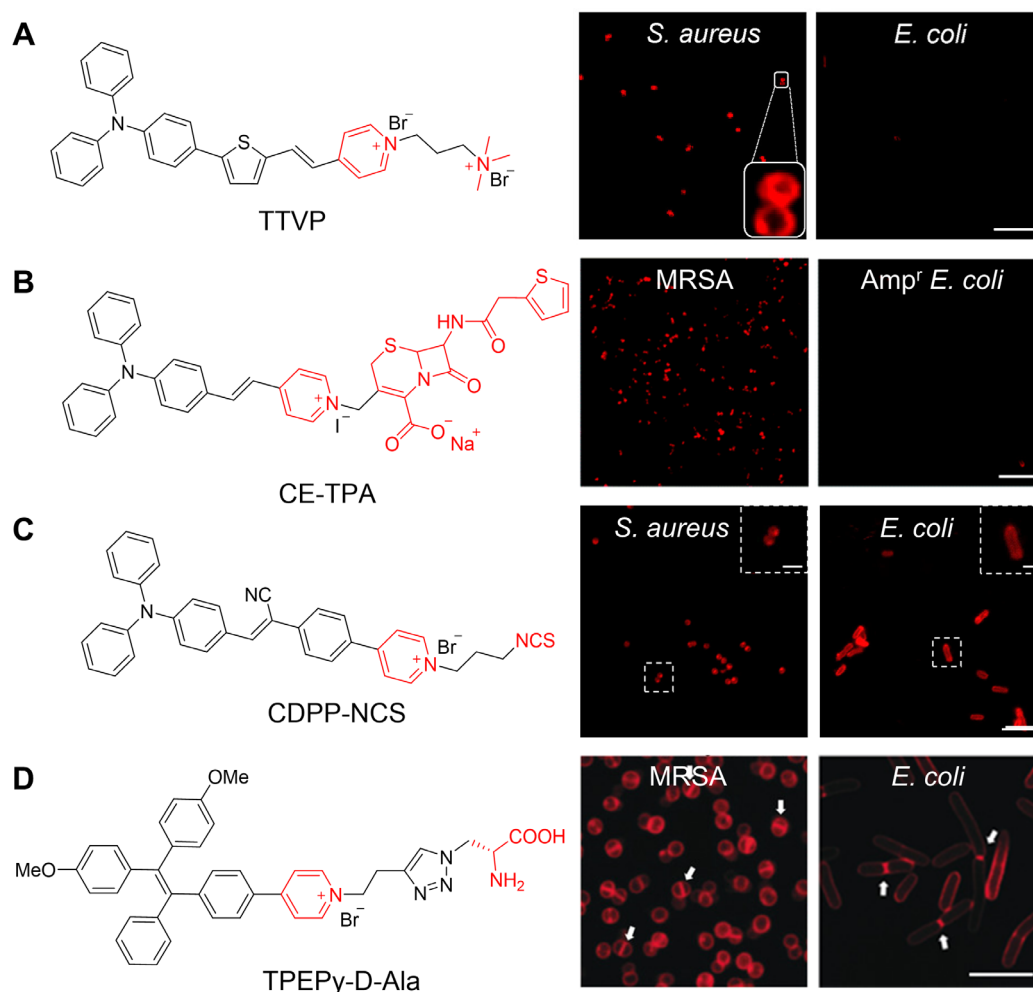
Figure 3. Different bacteria labeling strategies. (A) Charge-based labeling strategy. Scale bar: 10 μm. Reproduced from Ref. [41] with permission of Elsevier, © 2019. (B) Receptor-targeting labeling strategy. Scale bar: 10 μm. Reproduced from Ref. [34] with permission of the Royal Society of Chemistry, © 2022. (C) Isothiocyanate-based clickable covalent labeling strategy. Scale bar: 10 μm. Inset: scale bar: 2 μm. Reproduced from Ref. [47] with permission of Elsevier, © 2022. (D) Metabolic labeling strategy. Scale bar: 5 μm. Reproduced from Ref. [48] with permission of Wiley-VCH, © 2019.

The selective imaging capability of AIEgens endow them more interesting applications. Zhao et al. designed a TPE derivative modified with boric acid (TPE-2BA) for monitoring bacterial viability, which potentially could be used for the evaluation of bacterial drug sensitivity [49]. Interestingly, TPE-2BA can show strong fluorescence via passing through the compromised membrane of dead bacteria and binding with DNA inside. Differentiation of bacteria is one of the most important issues for rapid diagnosis and precise treatment in clinic [50-52]. It is reported that the cell envelope structures of Gram-negative (G−) bacteria, Gram-positive (G+) bacteria and fungi are different (Fig.

4A) [53, 54]. Zhou et al. successfully developed a microenvironment-sensitive AIE probe (IQ–Cm) for fast discrimination of G− bacteria, G+ bacteria and fungi by naked eyes (Fig. 4B–C) [55]. IQ–Cm has a twisted donor–acceptor structure and shows twisted intramolecular charge transfer (TICT) characteristics with a sensitive fluorescence color response to the microenvironment of pathogens. Driven by the intrinsic structural distinctions of the above-mentioned pathogens, the positive-charged IQ–Cm can stain the pathogens and selectively locate in different sites, leading to the naked-eye discernible emission colors. Therefore, IQ–Cm can directly discriminate the three pathogens via fluorescence, providing a promising platform for rapid pathogen detection and point-of-care diagnosis.

To achieve more rapid and reliable differentiation of pathogens, a series of simple and reliable sensor arrays based on TPE derivatives (TPE-ARs) are successfully developed by Zhou et al. for high-throughput pathogens screening [56]. As shown in Fig. 4D, all TPE-ARs had a cationic ammonium unit but different calculated oil-water separation coefficient (Clog$P$, n-octanol/water partition coefficient) (3~7), which correlated with their hydrophobic side chains. The Clog$P$ value could be used to evaluate the electrostatic and hydrophobic interaction between AIE probes and pathogens. Each TPE-AR shows fluorescence response after incubation with different pathogens due to the specific interaction, and vice versa. Then, the fluorescence pattern was analyzed by linear discriminant analysis (LDA), followed by identification results (Fig. 4E). These sensor arrays can identify diverse pathogens, even normal and drug-resistant bacteria or blends of pathogens, with nearly 100% accuracy. This system verifies that the AIE probes can perfectly meet the actual demand of the high throughput clinical screening and medical observation. Additionally, a more sensitive high-throughput sensor array composed of TPE derivatives with varied numbers of cationic side chains was constructed recently, which could detect and discriminate various bacteria at low concentrations down to 1×10^3 CFU mL^{-1}.
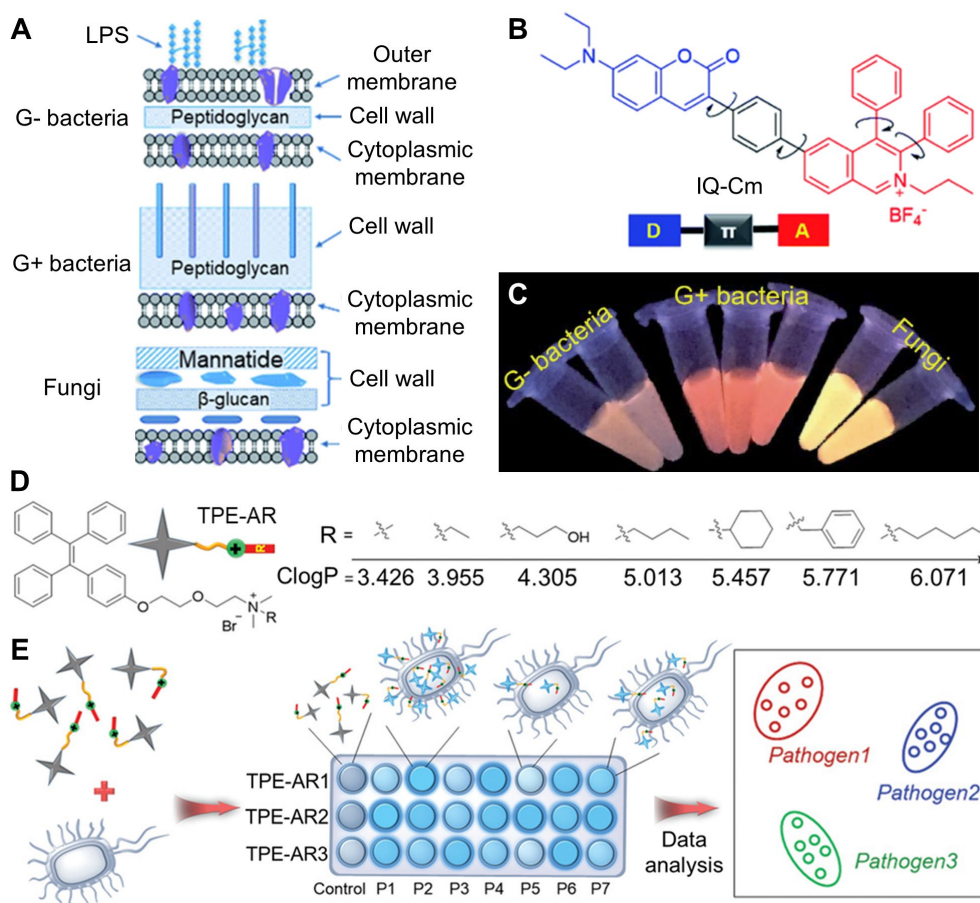
Figure 4. Differentiation of pathogens. (A) Schematic of cell envelope structures of Gram-negative (G−) bacteria, Gram-positive (G+) bacteria and fungi. (B) Chemical structure of IQ–Cm, an AIEgen with twisted intramolecular charge transfer (TICT) characteristics. (C) Photographs of IQ–Cm with different pathogens in PBS solutions obtained under 365 nm irradiation. Reproduced from Ref. [55] with permission of Royal Society of Chemistry, © 2020. (D) Structure of TPE-ARs with various ClogP values. (E) Schematic illustration of a sensor array composed of three TPE-ARs to achieve pathogen identification. P1–P7 represent seven kinds of pathogens. Reproduced from Ref. [56] with permission of Wiley-VCH, © 2018.

3.2 AIE biomaterials for detection of viruses

Rapid, sensitive and accurate detection of highly contagious viruses (e.g. SARS-CoV-2) is urgently demanded for the prevention and control of virus pandemic [57, 58]. The advantages of AIEgen *i.e.* luminosity, photobleaching resistance and biocompatibility promote their applications in ultrasensitive detection of viruses [59-61]. Xiong et al. demonstrated a dual-modality readout immunoassay platform based on AIEgen for detecting of viruses [62]. The mechanism of dual-mode

detection of virus is shown in Figure 5. A water-soluble multifunctional AIEgen (TPE-APP) with an enzymatic cleavage group was designed. The probe can be hydrolyzed by alkaline phosphatase (ALP) to form water-insoluble TPE-DMA aggregate and a highly redox species. On one hand, the TPE-DMA aggregate is intensively fluorescent. One the other hand, the redox species could reduce silver ion to generate a silver nanoshell on the surface of AuNP (AuNP@AgNP) that leads to the blue shift of the localized surface plasmonic resonance (LSPR) peak of AuNPs, displaying a pronounced color change from red to yellow and further to brown, which can be differentiated by naked eyes. By further taking advantage of effective immunomagnetic enrichment, enterovirus 71 (EV71) virus, as an example, can be specifically detected with a limit of detection concentration down to 1.4 copies/μL under fluorescence modality and in a broad range from 1.3×10^3 to 2.5×10^6 copies/μL with naked eyes. Most importantly, EV71 virions in 24 real clinical samples are successfully diagnosed with 100% accuracy. Compared to the gold standard polymerase chain reaction (PCR) assay, this immunoassay platform is not only much more convenient and cheaper, but also show excellent quantitatively capability, high sensitivity and strong anti-interference ability, paving great prospect for handy preliminary screening and high-accuracy in clinical diagnosis of viruses.
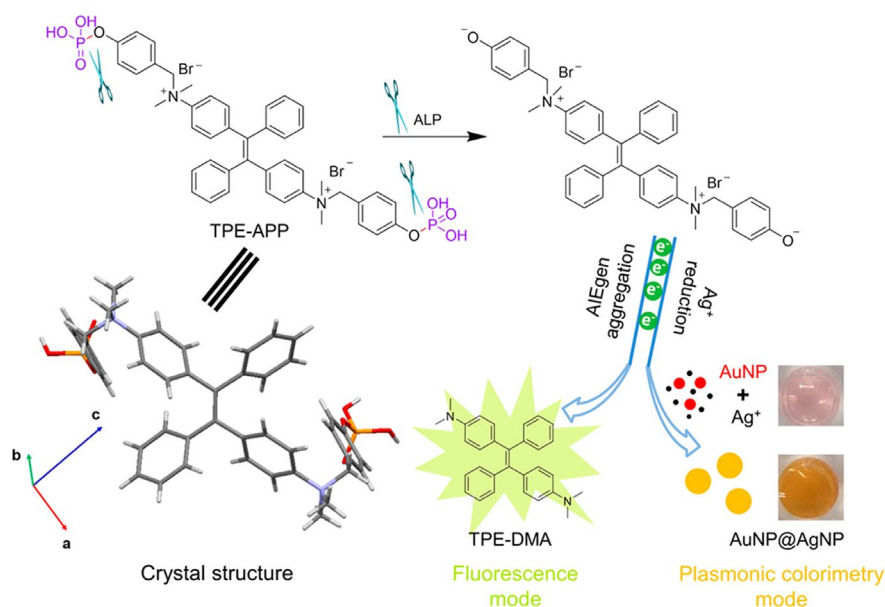

Figure 5. AIE materials for virus detection. Schematic illustration of fluorescent and plasmonic colorimetric dual-modality for virus detection based on a multifunctional AIEgen TPE-APP. Reproduced from Ref. [62] with permission of American Chemical Society, © 2018.

In addition to directly sensing viruses, AIEgens have also been applied in the detection of viral

proteins. Viral antigen-based detection could be developed as a complementary screening strategy for early diagnosis of SARS-CoV-2 infection. SARS-CoV-2 consists of four structural proteins, known as spike (S), envelope (E), membrane (M), and nucleocapsid (N) proteins [63]. Among them, N protein has been identified as one of the best early diagnostic targets and could be detected before the appearance of antibody in serum [64, 65]. Furthermore, the receptor binding domain (RBD) of S protein could be directly tested without virus lysis, which could act as a suitable diagnostic epitope [66]. Recently, Zhang et al. developed a wearable lateral flow test strip based on AIEgens for rapid detection of SARS-CoV-2 RBD protein and N protein (Fig. 6) [67]. Compared with the antigen test based on colloidal gold or fluorescein isothiocyanate (FITC), this testing platform provides higher sensitivity and specificity, stronger anti-inference ability, and desirable reproductivity with simple preparations. As shown in Fig. 6A, the N-hydroxysuccinimide (NHS) activated AIEgen reacts with antibody to produce AIEgens-labeled antibody. The test strip was composed of a PVC backing card, sample pad, nitrocellulose (NC) membrane, and absorption pad (Fig. 6B). The working mechanism of the strip was also shown in Fig. 6B. In general, for the detection antibody without binding reaction with the target antigen, it passed through the T line and bound to the secondary antibody on the control (C) line, bright fluorescent signal could be easily observed under 365 nm UV light irradiation with naked eyes. Due to the high brightness and anti-bleaching ability in aqueous solution, the detection limit can be as low as 6.9 ng/mL for RBD protein and 7.2 ng/mL for N protein, respectively. Therefore, this AIEgen-based strip presented excellent testing performance and thus could be built as a promising platform for rapid and accurate virus detection during the pandemic.
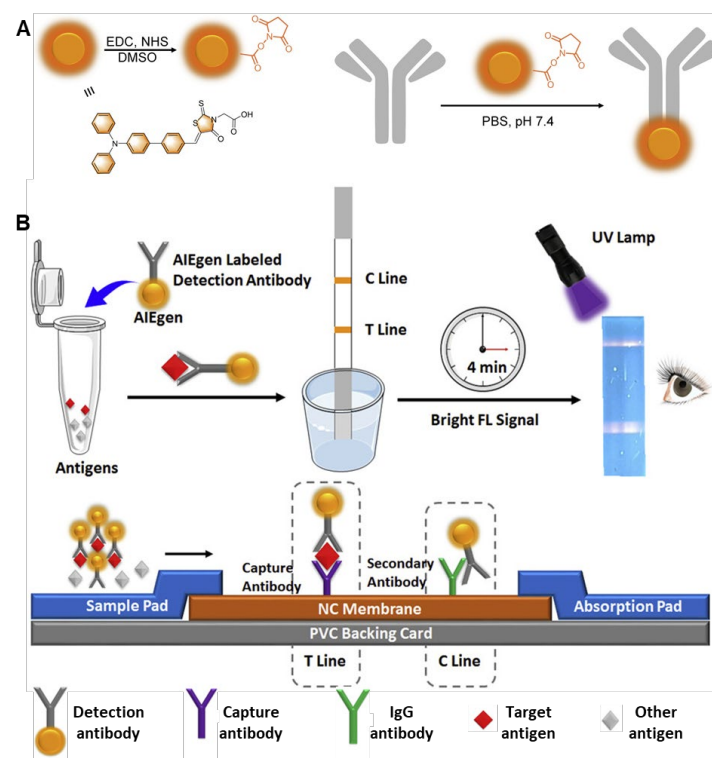
Figure 6. AIE materials for detection of viral protein. (A) Schematic of the preparation of NHS modified AIEgen and the antibody labeling with AIEgen. (B) Schematic of the general test strip platform based on AIEgens as a reporter for SARS-CoV-2 antigen detection. Reproduced from Ref. [62] with permission of American Chemical Society, © 2018.

3.3 AIE biomaterials for imaging of fungi

Fungi, a type of eukaryotes, are pathogenic to humans [68]. It is reported that fungi-related infectious diseases have been emerging as an important public health problem [69]. Evaluation of fungal viability and antifungal susceptibility was considered as key factors for the inspection and treatment of fungi-related infection in clinic [70, 71]. Previous methods widely used for fungal viability test are time-consuming and labor-intensive, involving counting the colony-forming unites (CFUs) after incubation, and using methylene blue to stain and count dead cells [72-74]. In comparison, fluorescence imaging offers a more rapid and accurate method for fungi detection with the privileges of easier operation and higher sensitivity [75]. In recent years, AIEgens that could stain fungi have been widely developed [76, 77]. An AIE-active probe DPASI has been designed by Zheng's group for sensing fungal viability (Fig. 7A) [78]. This molecule is water-dispersible and could selectively stain dead *C. albicans* in a wash-free

manner within 5 minutes. With the help of DPASI, live and dead *C. albicans* could be easily differentiated in fluorescence channel (Fig. 7B). The rapid imaging of dead *C. Candida* cells with impaired cell wall could be ascribed to the efficient binding of DPASI with mitochondria. Therefore, this probe provides a facile and promising platform not only for the rapid detection of fungal viability, but also for the accurate screening of new antifungal drugs, which would greatly contribute to the fungal research.

Another AIE probe DMASP was developed for antifungal susceptibility testing (AFST), which has been verified to be the most valuable way to determine the *in vitro* effectiveness of antifungal agents in clinic (Fig. 7C) [79]. Mitochondria-specific DMASP can monitor the change of mitochondrial membrane potential (MMP) caused by non-specific cation influx of the hyperpolarized membrane. In the AFST of azoles (e.g. fluconazole and itraconazole), elevated MMP can be reflected by the enhancement of fluorescence intensity, indicating the increased accumulation of positive-charged DMASP into mitochondria. As a contrast, antifungal drugs 5-flucytosine (5-FC) displayed no fluorescence in DMASP-based AFST because their rapid and efficient killing effect to fungi weakened the binding of DMASP to fungi (Fig. 7D). What's more, DMASP-based AFST system could differentiate fungal resistance among clinical fungal isolates via evaluating the time resolved fluorescence intensity. Compared with the time-consuming clinical standard AFSTs, this method benefits the advantages of easy operation, real-time monitoring and quantitative analysis, displaying great contribution to the detection of possible drug-resistant fungal strains and the precise use of antimicrobials against fungal diseases.
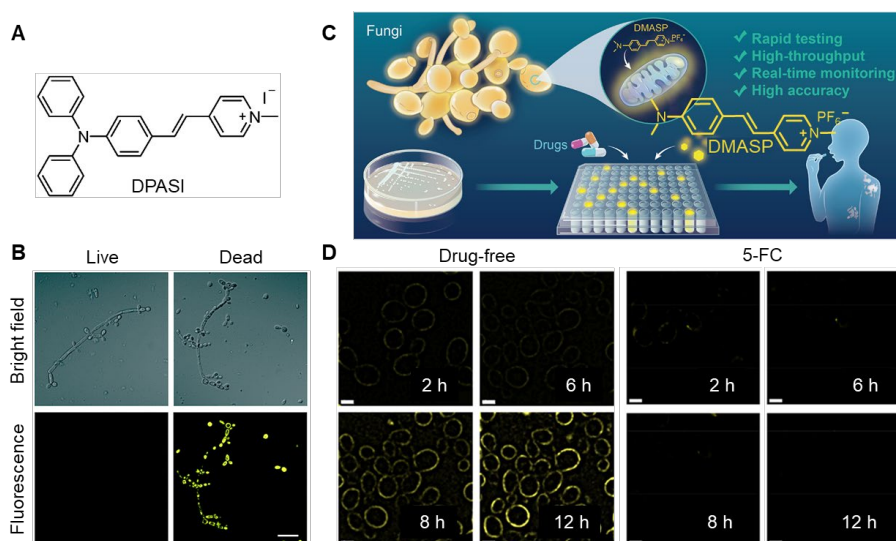
Figure 7. AIE materials for detection of fungal viability and susceptibility. (A) Molecular structure of DPASI. (B) Confocal laser scanning microscope (CLSM) images of *C. albicans* stained with DPASI. Reproduced from Ref. [78] with permission of the Royal Society of Chemistry and the Chinese Chemical Society, © 2020. (C) Schematic illustration of rapid and high-throughput testing of antifungal susceptibility using an AIEgen-based analytical system. (D) Structure illumination microscopy (SIM) fluorescence images of drug-free and 5-flucytosine (5-FC) treated *C. albicans* suspensions versus time. Scale bar = 6 μm. Reproduced from Ref. [79] with permission of Elsevier, © 2022.

4. AIE biomaterials for inactivation of pathogens

4.1 AIE biomaterials for inactivation of bacteria

Upon the detection of pathogenic bacteria, it is especially important to kill the pathogenic bacteria efficiently. In this section, different methods based on AIE biomaterials for bacterial inactivation will be presented, including AIE antibiotics, photodynamic therapy (PDT) and photothermal therapy (PTT) [80-83].

4.1.1 Antibiotics derivatives with AIE characteristics

Since penicillin was discovered in 1928, antibiotics have been widely used all over the world [8, 84]. Due to antibiotic abuse, multidrug-resistant (MDR) bacteria can evade antibiotics and thus have become a great threat to human health. Hence, production of new antibiotics is highly desirable [85, 86]. Pharmacologists usually focus on the structure-activity relationships of antibiotics to enhance their activity, with their optical properties ignored. In fact, investigating their photophysical properties is of great significance to understand their working mechanism [87]. It is reported that fluorescent antibiotic and its derivatives have great potential to become a new research tool to fight antibiotic resistance.

Recently, Wang et al. studied the AIE properties of several FDA-approved fluoroquinolone antibiotics (norfloxacin (NOR), levofloxacin (LEV), and moxifloxacin hydrochloride (MXF-HCl)) [88, 89]. After a systematical structure-activity relationship study, MXF modified with a

triphenylphosphonium (MXF-P) was successfully prepared with AIE feature and comparable antibacterial activity to MXF (Fig. 8A and 8B), which could be applied for rapid imaging of bacteria. Furthermore, MXF-P exhibited admirable antibacterial activity *in vitro* and *in vivo* by inhibition of bacterial division and destruction of the envelope structure (Fig. 8C). Similarly, Xie et al. developed a series of AIE active ciprofloxacin derivatives for bacterial theranostics based on pure nanodrugs (PNDs) strategy (Fig. 8D–8F) [90]. The nanoaggregates of ciprofloxacin derivatives showed excellent fluorescent properties with up to 11% quantum yield. Then, the antibacterial activities of the nanoaggregates were compared with molecular drugs. As shown in Fig. 8G, the nanoaggregate generally showed much better antibacterial activity than the soluble form with much lower minimal inhibit concentrations (MICs), demonstrating that nanodrug could enhance antibacterial activity of the molecular drug. These works provide an innovative strategy for new multifunctional drug discovery based on new use of old drug principle.
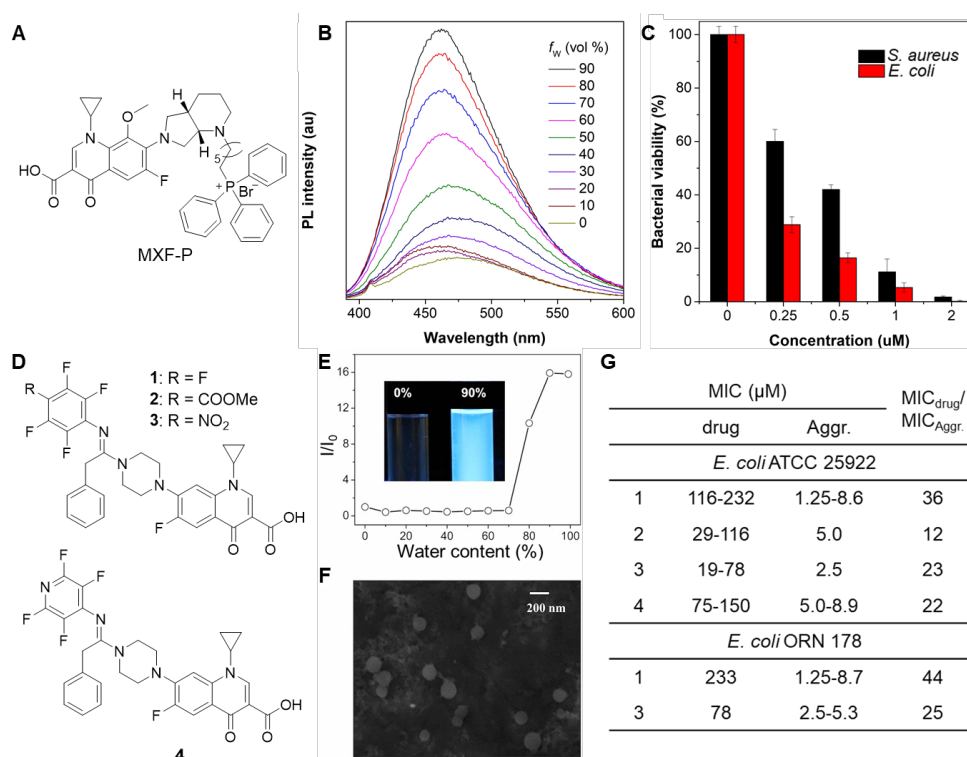

Figure 8. Antibiotics derivatives with AIE characteristics. (A) Chemical structure of moxifloxacin derivative MXF-P. (B) PL spectra of MXF-P in water/DMSO mixtures with different water fraction. (C) Antibacterial activity against bacteria of MXF-P at different concentrations. Reproduced from Ref. [88] with permission of Elsevier, © 2022. (D) Chemical structures of ciprofloxacin derivatives with AIE property. (E) Plot of relative emission intensity at 457 nm for 1 against water content in

water/MeCN mixtures. I_0: emission intensity at 0 vol % water. (F) SEM image of 1 prepared from 90 vol% water/MeCN. (G) Minimum inhibitory concentration (MIC) of the ciprofloxacin derivatives against *E. coli*. Reproduced from Ref. [89] with permission of National Academy of Sciences, © 2017.

4.1.2 Natural compounds with AIE property and photodynamic activity

In addition to modification of antibiotics, some multifunctional natural products with AIE properties have been applied for bacteria inactivation [91]. Lately, Michelle et al. report an AIE active natural compound Tanshinone IIA and investigated its application in photodynamic eradication of biofilm (Fig. 9) [92]. Tanshinone IIA is a traditional Chinese medicine and it chemical structure is shown in Fig. 9A. The photophysical properties were well characterized (Fig. 9B). Tanshinone IIA could efficiently generate ROS under white light irradiation (Fig. 9C). Furthermore, it was found that Tanshinone IIA could specifically stain bacterial biofilms, remarkably promote bacterial aggregation and photodynamic eradication of biofilm (Fig. 9D).
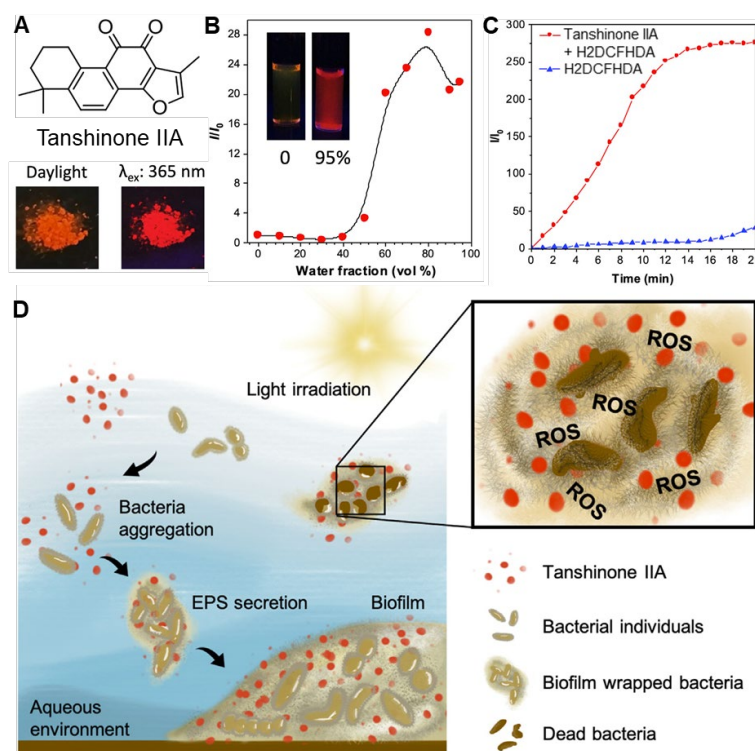

Figure 9. Natural product with AIE property and photodynamic activity. (A) Chemical structure of Tanshinone IIA and its photographs under daylight and 365 nm irradiation. (B) The plot of the emission maximum and the relative emission intensity (I/I_0) versus the composition of the

DMSO/water mixtures of Tanshinone IIA. Inset: fluorescence photographs of Tanshinone IIA in DMSO and in DMSO/water mixtures with 95% water fraction taken under 365 nm UV irradiation. (C) ROS generation of Tanshinone IIA upon white-light irradiation. (D) Schematic illustration of Tanshinone IIA for simultaneous targeting and photodynamic eradication of bacterial biofilms. Reproduced from Ref. [92] with permission of Elsevier, © 2022.

4.1.3 AIE biomaterials for photodynamic inactivation of bacteria

Rapid wound dressing and effective antibacterial therapy are of extreme importance for skin wounds treatment in emergency [93, 94]. By combing the advantages of in situ electrospinning and AIE PSs, Zhao et al. developed a feasible and rapid strategy for wound infection treatment of surgery or accident injuries by in situ depositing AIEgen based nanofibrous dressing (Fig. 10A) [95]. In their approach, AIEgens (TBP)-incorporated poly(ε-caprolactone) (PCL) solution could be readily electrospun by a handheld electrospinning device to form the nanofibrous dressing, which was closely and well adhesive to the wound surface. *In vitro* (Fig. 10B) and *in vivo* (Fig. 10C) experiments demonstrated that the AIE nanofibrous dressing exhibited excellent antibacterial activities and greatly promoted the wound healing process. Thus, the strategy of in situ deposition of AIE nanofibrous dressing via handheld electrospinning device can provide personalized therapies for emergency wounds with the advantages of convenience, versatility and universality.
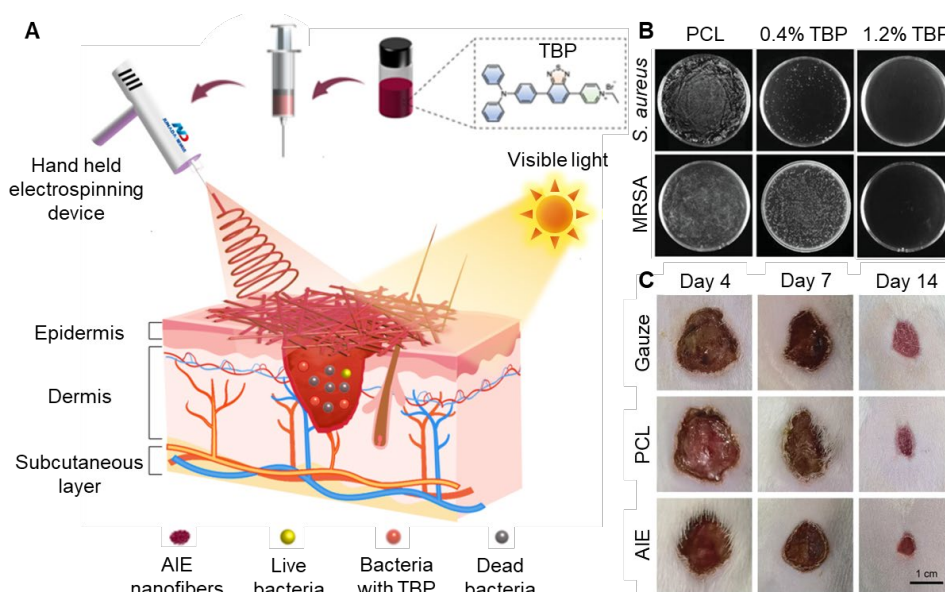

Figure 10. AIE materials for bacterial photodynamic therapy. (A) Schematic illustration of

electrospinning AIEgen TBP-incorporated antibacterial dressing. (B) Photos of *S. aureus* and MRSA treated with different TBP contents of TBP/PCL nanofibers upon white light irradiation (16 mW/cm^2) for 20 min.(C) Photographs of the appearance of the wounds after different treatment. Reproduced from Ref. [95] with permission of Wiley-VCH, © 2022.

In addition to explore the applications of AIE PS in different scenarios, researchers also devote a lot to elucidate the relationship of structure and function relationship of antibacterial agents to achieve accurate and efficient antibiosis [96]. Kang et al. designed a family of positively charged PSs with AIE feature [97]. By adjusting the Clog*P* value (3~5), these positively charged AIEgens could selectively stain G+ bacteria without any extra targeting groups. Benefiting from the excellent specificity to G+ bacteria, effective ROS generation ability, and bright NIR emission, these AIEgens were successfully utilized for the selective photodynamic theranostics of *S. aureus*. This successful example on structure-activity relationship study could provide guidance for the further exploration of novel antibacterial theranostic agents.

4.1.4 AIE biomaterials for photothermal inactivation of bacteria

Biofilm-related infections, such as dental plaque and bone implant, have brought great suffering to patients and heavy financial burden to society [98, 99]. Bacterial biofilm is a unified community where bacteria are encapsulated by the matrix, leading to the resistance to antibiotics [100]. PTT has been widely studied as one of the most attractive strategies for combating bacteria with its advantages on light-controllability and hardly no drug resistance [83, 101]. Recently, He et al. report a highly efficient photothermal nanoparticle (TN NP to eradicate biofilms (Fig. 11) [102]. TN NPs were prepared by encapsulation of NIR-absorbing photothermal AIEgens (2TPE-2NDTA-02) with DSPE-PEG$_{2000}$ (Fig. 11A). By taking advantage of active intramolecular motions in the aggregate state and enhanced molar absorptivity, TN NPs showed high ability in photothermal conversion and excellent photobleaching resistance. Under 808 nm NIR laser irradiation, the temperatures of the aqueous solutions elevated with time and saturated within 3 minutes (Fig. 11B). The prepared NPs can effectively eliminate mature *S. aureus* biofilms upon NIR laser by destruction of the adjacent bacteria and deactivation of the adhesive components (Fig. 11C–D). Therefore, PTT is one of the most promising potential candidates for the clinical treatment of biofilm in the future.
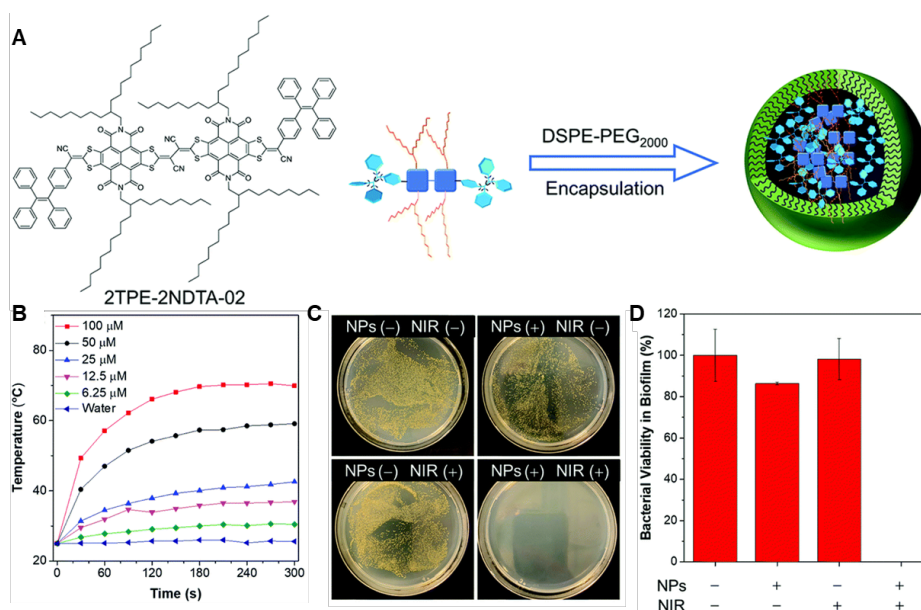
Figure 11. AIE materials for bacterial photothermal therapy. (A) Schematic illustrations of fabrication of TN NPs by encapsulating DSPE-PEG$_{2000}$ with 2TPE-2NDTA-02. (B) Photothermal conversion behavior of TN NPs in aqueous solution at different concentrations (0–100 μM) under 808 nm laser irradiation. (C) Photographs of bacteria colonies grown on NB agar. (D) Relative bacterial viability in the treated biofilm of each group. Reproduced from Ref. [102] with permission of the Royal Society of Chemistry, © 2021.

4.1.5 AIE materials for bacterial photodynamic/photothermal synergistic therapy

Some AIEgens have been developed with synergistic PDT and PTT effect [103, 104]. For instance, Li et al. developed an AIEgens-loaded mask with sunlight-triggered photodynamic/photothermal anti-bacterial functions by utilizing AIEgen based nanofibrous membrane (TTVB@NM) (Fig. 12A) [105]. Under simulated sunlight irradiation, TTVB@NM exhibited efficient ROS generation and moderate photothermal conversion performance (Fig. 12B–C). Furthermore, TTVB@NM was covered on a medical mask and displayed efficient antimicrobial activity against pathogenic aerosols (Fig. 12D). It is notable that the filtration efficiency and air permeability of the TTVB@NM coated mask showed comparable even better performance than that of other reported antimicrobial wearable materials.
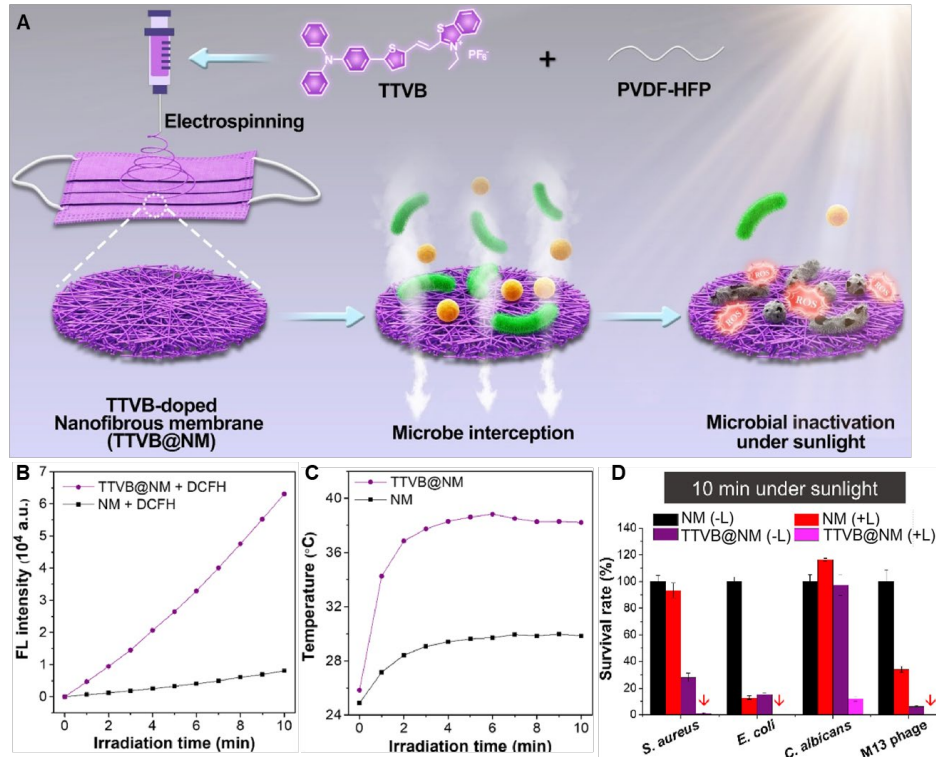
Figure 12. AIE materials for bacterial photodynamic/photothermal synergistic therapy. (A) Schematic illustration of the preparation of TTVB-loaded nanofibrous membrane (TTVB@NM) through electrospinning for microbial inactivation under sunlight. (B) ROS generation of TTVB@NM under the irradiation of simulated sunlight. (C) The photothermal conversion performance of NM and TTVB@NM under the irradiation of simulated sunlight. (D) Survival rates of different microbes after sunbathing. (Red arrows: antimicrobial efficacy is around 100%). Reproduced from Ref. [105] with permission of Elsevier, © 2021.

4.2 AIE biomaterials for inactivation of fungi

Fungus is a common microorganism widely found in nature, which can lead to various severe infections, like fungal keratitis, fungal dermatosis, and so on [106, 107]. The treatment of fungi-related infectious diseases is still challenging because current antifungal drugs suffer drug resistance and side effects. Recently, some AIEgens with PDT activity are reported as promising candidates for the treatment of fungal infections with the advantages of negligible drug resistance, high spatiotemporal accuracy, and low side effects [108].

Fungal keratitis is a widespread disease which would cause corneal tissue injury and sight-threatening complication [106]. Mitochondria is considered as an ideal target for fungi inactivation

due to its important role in fungi morphogenesis virulence and drug resistance [109]. As such, selectively targeting fungal mitochondria is a valuable approach for fungi treatment with low side effects [110]. Zhou et al. developed a series of mitochondria-specific isoquinolinium (IQ)-based AIEgens (IQ-TPE-2O, IQ-Cm, and IQ-TPA) for selectively photodynamic killing of fungi and effective treatment of keratitis (Fig. 13A) [111]. Driven by the intrinsic discrepancy in surface membrane potential between fungi and mammalian cells and negative mitochondrial membrane potential (MMP), these cationic AIEgens designed with proper hydrophobicity were expected to preferentially accumulate in the mitochondria of fungi over mammalian cells and cause mitochondrial disruption by PDT effect (Fig. 13B). The results indicate that all three AIEgens, especially IQ-TPA, exhibit excellent antifungal activity for *in vivo* treatment, which is much better than the clinically used photosensitizer rose bengal (Fig. 13C).

Adjusting the alkyl chain lengths can modulate the interaction between AIEgens and fungi to improve the treatment effect. Li et al. developed a family of cationic AIEgens with numerous alkyl chain lengths for anti-fungal therapy [112]. Among them, TPA-S-C6-NMe$_3^+$ can interact with fungi through electrostatic and hydrophobic interactions. The synergistic effect of alkyl chain length, the ability of ROS generation, and amphiphilicity endow TPA-S-C6-NMe$_3^+$ superior anti-fungi photodynamic activity than commercial PSs, e.g., methylene blue, chlorin e6, and protoporphyrin IX. Furthermore, TPA-S-C6-NMe$_3^+$ was applied for *in vivo* wound healing, which not only showed an excellent antimicrobial activity but also promoted the regeneration of new blood vessels and fibroblasts in infected tissues.
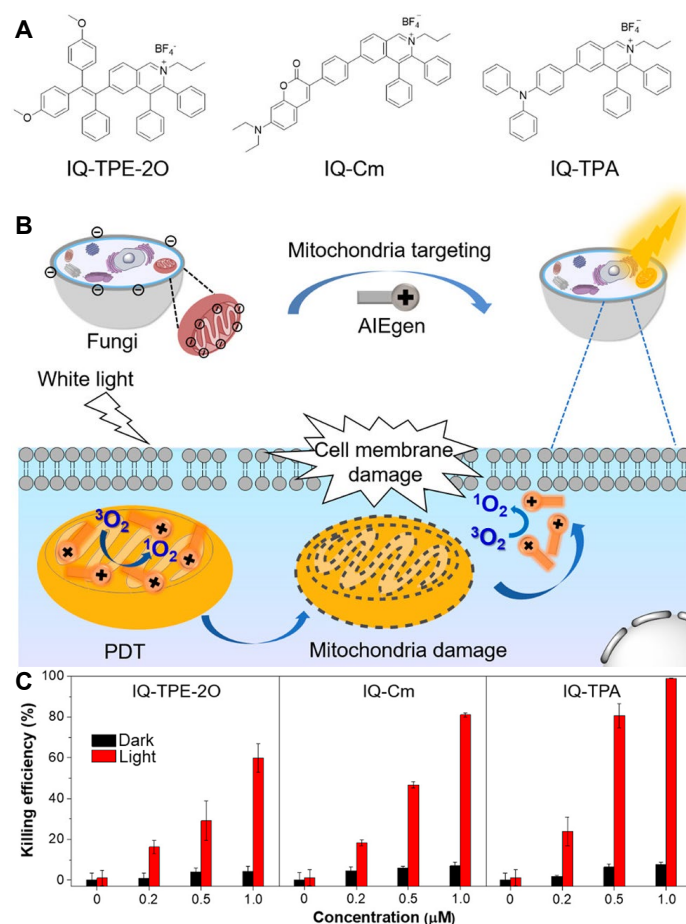
Figure 13. AIE materials for selective photodynamic killing of fungi. (A) Molecular structure and (B) schematic illustration of AIEgens for selective mitochondria-specific PDT of fungi. (C) Antifungal activity of AIEgens toward *C. albicans* at different concentrations in the dark and under white light irradiation. Reproduced from Ref. [111] with permission of American Chemical Society, © 2021.

4.3 AIE biomaterials for inactivation of virus

Besides bacterium and fungus, virus is another great threat to public health. There are numerous barriers in the prevention and control of virus-related pandemics due to the lack of specific drugs. Personal protective equipment (PPE), like masks and protective suits, is a key factor to inhibit the spread of virus, preventing healthy people especially frontline healthcare doctors and nurses from virus infection [113]. Due to poor self-virucidal capabilities of traditional PPEs, viruses accumulate on the fibers of PPEs over long-term usage, leading to wearers' infection. In addition, conventional PPEs are usually disposable with limited service life [114]. Further, the improper disposal of PPEs is likely to cause cross-contamination [115]. Therefore, there is an emergency to develop self-

antiviral PPEs with long-term usable and reusable characteristics.

A series of AIE PS based PPEs with real-time self-antiviral capabilities has been successfully repoted recently (Fig. 14) [116]. For instance, the AIEgen ASCP-TPA was synthesized with the advantages of facile synthesis, excellent biocompatibility, and superior ROS generation ability. ASCP-TPA-attached fabrics could efficiently inactivate SARS-CoV-2 within 10 minutes under ultralow-power visible light irradiation (3.0 mW/cm^2). Moreover, the modified fabrics not only showed low toxicity to normal cell but also displayed highly durable anti-virus properties despite of 100 washings or exposure to office light for 2 weeks. This strategy shows a great potential to fight against SARS-CoV-2 or other airborne pathogens and to improve global PPE supply shortages.
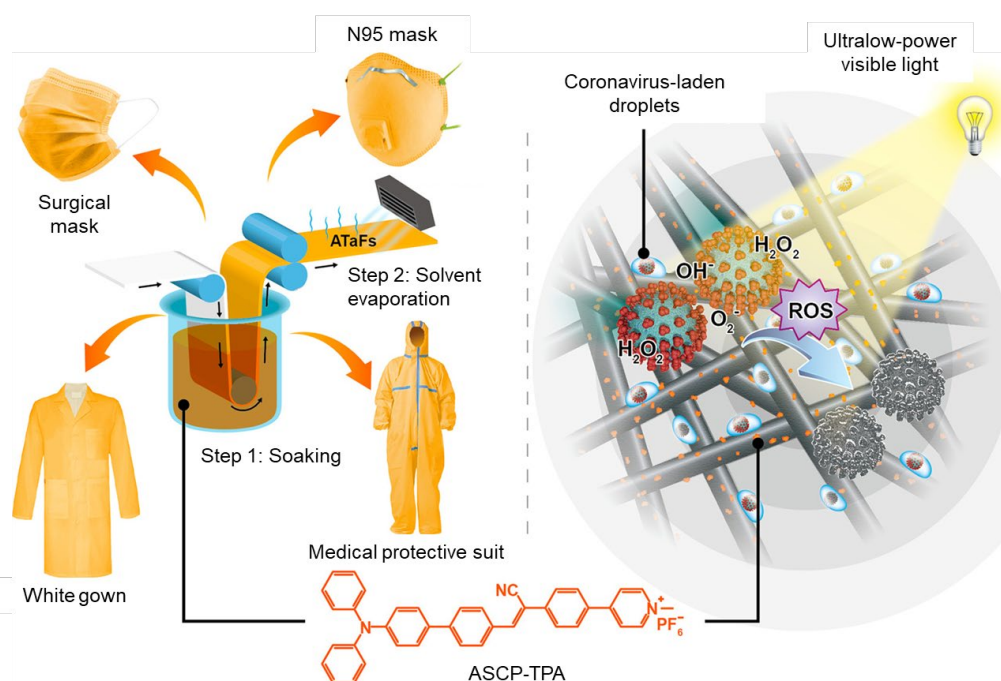

Figure 14. AIE materials for self-antiviral personal protective equipments (PPEs). Schematic diagram of the preparation of ASCP-TPA-attached fabrics (ATaFs) and various ATaF-based PPEs (left) and the photodynamic inactivation principle of ATaFs against coronavirus upon ultralow-power light irradiation (3.0 mW/cm^2) (right). Reproduced from Ref. [118] with permission of American Chemical Society, © 2021.

Multifunctional AIE biomaterials with antiviral and anti-inflammatory abilities is highly desirable. To date, cell membrane-coated nanoparticles (NPs) have emerged as a biomimetic nanomedicine platform for treatment of different diseases [117]. Based on this bioinspired strategy, Li et al. developed a type of multifunctional photothermal nanoparticles coated by alveolar macrophage

(AM) membrane to kill coronavirus [118]. The AM membranes endow NPs with function as the coronavirus receptor and multiple cytokine receptors for coronavirus cellular entry and various proinflammatory cytokine binding, respectively, to keep the virus away from their host targets. After treatment of a surrogate mouse model of COVID-19 caused by murine hepatitis virus A-59 (MHV-A529) with these multifunctional AM-bioinspired NPs under NIR irradiation, not only the virus burden and cytokine levels in lungs decreased but also tissue damage and inflammation were relieved and improved. Moreover, the viral transmission and infection progress can be restricted after PTT. This work provides an ideal strategy to fabricate novel multifunctional bioinspired NPs with cell membrane-coating method for the effective treatment of COVID-19.
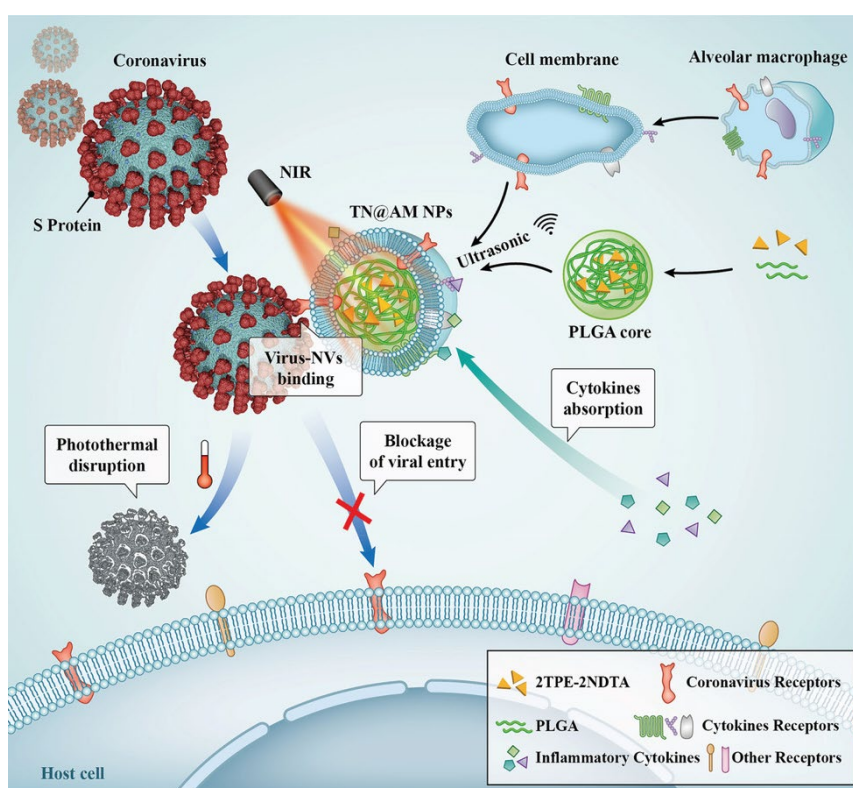

Figure 15. AIE materials for photothermal disruption of virus. Schematic illustration of multifunctional alveolar macrophage-like nanoparticles for coronavirus cellular entry blockage, virus photothermal disruption, and inflammatory cytokines absorption. Reproduced from Ref. [118] with permission of Wiley-VCH, © 2021.

In addition to photothermal reagents, AIEgens are also utilized for viral photodynamic inactivation. Recently, Wu et al. reported a new AIEgen (DTTPB) for highly efficient photodynamic inactivation of human coronavirus [119]. DTTPB with a hydrophilic head and two hydrophobic tails can selectively bind the envelope of human coronavirus. Under low power white light irradiation (9

mW/cm^2), DTTPB showed excellent antiviral effect on human coronavirus. These AIEgens could target the viral phospholipid bilayers or protein covering viral capsid via the lipophilic cations of IQ, thus destroy the viral structure under white light irradiation.

5. Summary and outlook

In the past 20 years, AIEgens-based applications have been extensively developed, especially in biomedical field, including biosensing, bioimaging, cancer theranostics, microbe inactivation, and so on. This review aims to highlight the latest advances of AIEgens-based biomaterials for theranostics of bacteria, fungi and viruses. Based on the nature of these three pathogens, AIEgens are well modified and thus endowed with the capability of pathogen differentiation and selective imaging. Integrated with chemotherapeutic activity or phototherapeutic activity, multifunctional AIE biomaterials are developed for efficient pathogen inactivation.

Although AIEgens-based antimicrobial theranostics have made a remarkable progress, there are still much room for improvement. (1) Visualization of interactions of bacteria-bacteria, microbe-bacteria plays an important role in understanding the corresponding physiological processes. To date, several NIR dyes have been developed for covalent binding with bacteria based on metabolic labeling strategy [120]. As a result, the endocytosis of bacteria, the interaction of gut microbiota, and other dynamic processes could be real-time monitored. (2) Artificial intelligent (AI) assisted pathogen differentiation can significantly improve the accuracy, rapidity and sensitivity, which is highly suitable for high-throughput assay. (3) The back-to-basics principle of new uses of old drugs has emerged as a fruitful basis for the discovery of new AIE drugs [121]. Thus, some AIE-active natural compounds with advantages of biocompatibility, biodegradability, and intrinsic pharmacological activity, have been developed for various applications. (4) Biosafety is a frequently discussed topic, which is an essential factor to advance the clinical application. To date, the excretion of AIE NPs in hepatobiliary and gastrointestinal pathway of non-human primates and rodents has been investigated [122]. More studies on AIE biomaterials, such as bio-distribution and pharmacokinetics, need to be conducted in future.

Conflicts of interest statement.

The author declares no conflict of interest.

References:

1. Dobson AP, Carper ER. Infectious diseases and human population history. *BioScience* **1996**;46:115–126.

2. Singh SR, Krishnamurthy NB, Mathew BB. A review on recent diseases caused by microbes. *J Appl Environ Microbiol* **2014**;2:106–115.

3. Dong E, Ratcliff J, Goyea TD, Katz A, Lau R, Ng TK, Garcia B, Bolt E, Prata S, Zhang D, Murray RC, Blake MR, Du H, Ganjkhanloo F, Ahmadi F, Williams J, Choudhury S, Gardner LM. The johns hopkins university center for systems science and engineering COVID-19 dashboard: Data collection process, challenges faced, and lessons learned. *Lancet Infect Dis* **2022**;22:e370–e376.

4. Bartholomew JW, Mittwer T. The Gram stain. *Bacteriol Rev* **1952**;16:1–29.

5. DeFarge C, Trichet J, Jaunet A-M, Robert M, Tribble J, Sansone FJ. Texture of microbial sediments revealed by cryo-scanning electron microscopy. *J Sediment Res* **1996**;66:935–947.

6. Lasken RS, McLean JS. Recent advances in genomic DNA sequencing of microbial species from single cells. *Nat Rev Genet* **2014**;15:577–584.

7. Levy SB, Marshall B. Antibacterial resistance worldwide: Causes, challenges and responses. *Nat Med* **2004**;10:S122–S129.

8. Hutchings MI, Truman AW, Wilkinson B. Antibiotics: past, present and future. *Curr Opin Microbiol* **2019**;51:72–80.

9. Johnson I, Spence MTZ, Eds. Molecular Probes Handbook, A Guide to Fluorescent Probes and Labeling Technologies, 11th ed. *Life Technologies Corporation,* **2010**.

10. Birks JB. Photophysics of aromatic molecules. *Wiley, London,* **1970**.

11. Luo J, Xie Z, Lam JW, Cheng L, Chen H, Qiu C, Kwok HS, Zhan X, Liu Y, Zhu D, Tang BZ. Aggregation-induced emission of 1-methyl-1,2,3,4,5-pentaphenylsilole. *Chem Commun* **2001**:1740–1741.

12. Mei J, Leung NL, Kwok RT, Lam JW, Tang BZ. Aggregation-induced emission: Together we shine, united we soar! *Chem Rev* **2015**;115:11718–11940.

13. Zhao Z, Zhang H, Lam JWY, Tang BZ. Aggregation-induced emission: New vistas at the aggregate level. *Angew Chem Int Ed* **2020**;59:9888–9907.

14. He W, Zhang Z, Luo Y, Kwok RTK, Zhao Z, Tang BZ. Recent advances of aggregation-induced emission materials for fluorescence image-guided surgery. *Biomaterials* **2022**;288:121709.

15. Kang M, Zhang Z, Song N, Li M, Sun P, Chen X, Wang D, Tang BZ. Aggregation-enhanced theranostics: AIE sparkles in biomedical field. *Aggregate* **2020**;1:80–106.

16. Chen X, Han H, Tang Z, Jin Q, Ji J. Aggregation-induced emission-based platforms for the treatment of bacteria, fungi, and viruses. *Adv Healthcare Mater* 2021:e2100736.

17. Balachandran YL, Jiang X. Aggregation-induced fluorogens in bio-detection, tumor imaging, and therapy: A review. *CCS Chem* **2022**;4:420–436.

18. Peng Q, Shuai Z. Molecular mechanism of aggregation-induced emission. *Aggregate* **2021**;2:e91.

19. Cai Y, Du L, Samedov K, Gu X, Qi F, Sung HHY, Patrick BO, Yan Z, Jiang X, Zhang H, Lam JWY, Williams ID, Lee Phillips D, Qin A, Tang BZ. Deciphering the working mechanism of aggregation-induced emission of tetraphenylethylene derivatives by ultrafast spectroscopy. *Chem Sci* **2018**;9:4662–4670.

20. Zhao Z, Zheng X, Du L, Xiong Y, He W, Gao X, Li C, Liu Y, Xu B, Zhang J, Song F, Yu Y, Zhao X, Cai Y, He X, Kwok RTK, Lam JWY, Huang X, Lee Phillips D, Wang H, Tang BZ. Non-aromatic annulene-based aggregation-induced emission system via aromaticity reversal process. *Nat Commun* **2019**;10:2952.

21. Park H, Niu G, Wu C, Park C, Liu H, Park H, Kwok RTK, Zhang J, He B, Tang BZ. Precise and long-term tracking of mitochondria in neurons using a bioconjugatable and photostable AIE luminogen. *Chem Sci* **2022**;13:2965–2970.

22. Jiang M, Gu X, Lam JWY, Zhang Y, Kwok RTK, Wong KS, Tang BZ. Two-photon AIE bio-probe with large Stokes shift for specific imaging of lipid droplets. *Chem Sci* **2017**;8:5440–5446.

23. Gao M, Tang BZ. Fluorescent sensors based on aggregation-induced emission: Recent advances and perspectives. *ACS Sens* **2017**;2:1382–1399.

24. Leung CW, Hong Y, Chen S, Zhao E, Lam JW, Tang BZ. A photostable AIE luminogen for specific mitochondrial imaging and tracking. *J Am Chem Soc* **2013**;135:62–65.

25. Liu H, Xiong LH, Kwok RTK, He X, Lam JWY, Tang BZ. AIE bioconjugates for biomedical applications. *Adv Opt Mater* **2020**;8:2000162.

26. Liu S, Feng G, Tang BZ, Liu B. Recent advances of AIE light-up probes for photodynamic therapy. *Chem Sci* **2021**;12:6488–6506.

27. Wang S, Wang X, Yu L, Sun M. Progress and trends of photodynamic therapy: From traditional photosensitizers to AIE-based photosensitizers. *Photodiagno Photodyn Ther* **2021**;34:102254.

28. Cai X, Liu B. Aggregation-induced emission: Recent advances in materials and biomedical applications. *Angew Chem Int Ed* **2020**;59:9868–9886.

29. Feng G, Zhang GQ, Ding D. Design of superior phototheranostic agents guided by Jablonski diagrams. *Chem Soc Rev* **2020**;49:8179–8234.

30. Kasha M. Characterization of electronic transitions in complex molecules. *Discuss Faraday Soc* **1950**;9:14–19.

31. Qian J, Tang BZ. AIE Luminogens for bioimaging and theranostics: From organelles to animals. *Chem* **2017**;3:56–91.

32. Xu S, Duan Y, Liu B. Precise molecular design for high-performance luminogens with aggregation-induced emission. *Adv Mater* **2020**;32:e1903530.

33. Lv F, Fan X, Liu D, Song F. Photothermal agents based on small organic fluorophores with

intramolecular motion. *Acta Biomater* **2022**;149:16–29.

34. Wan Q, Zhang R, Zhuang Z, Li Y, Huang Y, Wang Z, Zhang W, Hou J, Tang BZ. Molecular engineering to boost AIE-active free radical photogenerators and enable high-performance photodynamic therapy under hypoxia. *Adv Funct Mater* 2020;30:2002057.

35. Dai J, Wu X, Ding S, Lou X, Xia F, Wang S, Hong Y. Aggregation-induced emission photosensitizers: From molecular design to photodynamic therapy. *J Med Chem* **2020**;63:1996–2012.

36. Liu Z, Zou H, Zhao Z, Zhang P, Shan GG, Kwok RTK, Lam JWY, Zheng L, Tang BZ. Tuning organelle specificity and photodynamic therapy efficiency by molecular function design. *ACS Nano* **2019**;13:11283–11293.

37. Cohan FM. What are bacterial species? *Annu Rev Microbiol* **2002**;56:457–487.

38. Hu R, Zhou F, Zhou T, Shen J, Wang Z, Zhao Z, Qin A, Tang BZ. Specific discrimination of Gram-positive bacteria and direct visualization of its infection towards mammalian cells by a DPAN-based AIEgen. *Biomaterials* **2018**;187:47–54.

39. Silhavy TJ, Kahne D, Walker S. The bacterial cell envelope. *Cold Spring Harbor Perspect Biol* **2010**;2:a000414.

40. Shi X, Sung SHP, Chau JHC, Li Y, Liu Z, Kwok RTK, Liu J, Xiao P, Zhang J, Liu B, Lam JWY, Tang BZ. Killing G(+) or G(−) bacteria? The important role of molecular charge in AIE-active photosensitizers. *Small Methods* **2020**;4:2000046.

41. Lee MMS, Xu W, Zheng L, Yu B, Leung ACS, Kwok RTK, Lam JWY, Xu FJ, Wang D, Tang BZ. Ultrafast discrimination of Gram-positive bacteria and highly efficient photodynamic antibacterial therapy using near-infrared photosensitizer with aggregation-induced emission characteristics. *Biomaterials* **2020**;230:119582.

42. Welsh MA, Taguchi A, Schaefer K, Van Tyne D, Lebreton F, Gilmore MS, Kahne D, Walker S. Identification of a functionally unique family of penicillin-binding proteins. *J Am Chem Soc* **2017**;139:17727–17730.

43. Ding Y, Li Z, Xu C, Qin W, Wu Q, Wang X, Cheng X, Li L, Huang W. Fluorogenic probes/inhibitors of beta-lactamase and their applications in drug-resistant bacteria. *Angew Chem Int Ed* **2021**;60:24–40.

44. Wang C, Wang J, Xue K, Xiao M, Sun Z, Zhu C. A receptor-targeting AIE photosensitizer for selective bacterial killing and real-time monitoring of photodynamic therapy outcome. *Chem Commun* **2022**;58:7058–7061.

45. Dai T, Xie J, Zhu Q, Kamariza M, Jiang K, Bertozzi CR, Rao J. A Fluorogenic Trehalose probe for tracking phagocytosed mycobacterium tuberculosis. *J Am Chem Soc* **2020**;142:15259–15264.

46. Hu X, Zhao X, He B, Zhao Z, Zheng Z, Zhang P, Shi X, Kwok RTK, Lam JWY, Qin A, Tang BZ. A simple approach to bioconjugation at diverse levels: Metal-free click reactions of activated alkynes with native groups of biotargets without prefunctionalization. *Research* **2018**; 3152870.

47. Zhang Z, He W, Deng Z, Liu Y, Wen H, Wang Y, Ye Z, Kin Kwok RT, Qiu Z, Zhao Z, Tang BZ. A clickable AIEgen for visualization of macrophage-microbe interaction. *Biosens Bioelectron* **2022**;216:114614.

48. Hu F, Qi G, Kenry, Mao D, Zhou S, Wu M, Wu W, Liu B. Visualization and in situ ablation of intracellular bacterial pathogens through metabolic labeling. *Angew Chem Int Ed* **2020**;59:9288–9292.

49. Zhao E, Hong Y, Chen S, Leung CWT, Chan CYK, Kwok RTK, Lam JWY, Tang BZ. Highly

fluorescent and photostable probe for long-term bacterial viability assay based on aggregation-induced emission. *Adv Healthcare Mater* **2014**;3:88–96.

50. Procop GW. Molecular diagnostics for the detection and characterization of microbial pathogens. *Clin Infect Dis* **2007**;45:S99–S111.

51. Sanguinetti M, Posteraro B, Beigelman-Aubry C, Lamoth F, Dunet V, Slavin M, Richardson MD. Diagnosis and treatment of invasive fungal infections: looking ahead. *J Antimicrob Chemother* **2019**;74:ii27–ii37.

52. Tang YW, Procop GW, Persing DH. Molecular diagnostics of infectious diseases. *Clin Chem* **1997**;43:2021–2038.

53. Yuan H, Liu Z, Liu L, Lv F, Wang Y, Wang S. Cationic conjugated polymers for discrimination of microbial pathogens. *Adv Mater* **2014**;26:4333–4338.

54. Wang Y, Corbitt TS, Jett SD, Tang Y, Schanze KS, Chi EY, Whitten DG. Direct visualization of bactericidal action of cationic conjugated polyelectrolytes and oligomers. *Langmuir* **2012**;28:65–70.

55. Zhou C, Jiang M, Du J, Bai H, Shan G, Kwok RTK, Chau JHC, Zhang J, Lam JWY, Huang P, Tang BZ. One stone, three birds: one AIEgen with three colors for fast differentiation of three pathogens. *Chem Sci* **2020**;11:4730–4740.

56. Zhou C, Xu W, Zhang P, Jiang M, Chen Y, Kwok RTK, Lee MMS, Shan G, Qi R, Zhou X, Lam JWY, Wang S, Tang BZ. Engineering sensor arrays using aggregation-induced emission luminogens for pathogen identification. *Adv Funct Mater* **2019**;29: 1805986.

57. Smith PL, WalkerPeach CR, Fulton RJ, DuBois DB. A rapid, Sensitive, multiplexed assay for detection of viral nucleic acids using the FlowMetrix system. *Clin Chem* **1998**;44:2054–2056.

58. Parida MM. Rapid and real-time detection technologies for emerging viruses of biomedical importance. *J Biosci* **2008**;33:617–628.

59. Chen R, Ren C, Liu M, Ge X, Qu M, Zhou X, Liang M, Liu Y, Li F. Early detection of SARS-CoV-2 seroconversion in humans with aggregation-induced near-infrared emission nanoparticle-labeled Lateral Flow Immunoassay. *ACS Nano* **2021**;15:8996–9004.

60. Bian L, Li Z, He A, Wu B, Yang H, Wu Y, Hu F, Lin G, Zhang D. Ultrabright nanoparticle-labeled lateral flow immunoassay for detection of anti-SARS-CoV-2 neutralizing antibodies in human serum. *Biomaterials* **2022**;288:121694.

61. Wang G, Yang L, Li C, Yu H, He Z, Yang C, Sun J, Zhang P, Gu X, Tang BZ. Novel strategy to prepare fluorescent polymeric nanoparticles based on aggregation-induced emission via precipitation polymerization for fluorescent lateral flow assay. *Mater Chem Front* **2021**;5:2452–2458.

62. Xiong LH, He X, Zhao Z, Kwok RTK, Xiong Y, Gao PF, Yang F, Huang Y, Sung HH, Williams ID, Lam JWY, Cheng J, Zhang R, Tang BZ. Ultrasensitive virion immunoassay platform with dual-modality based on a multifunctional aggregation-induced emission luminogen. *ACS Nano* **2018**;12:9549–9557.

63. Lu R, Zhao X, Li J, Niu P, Yang B, Wu H, Wang W, Song H, Huang B, Zhu N, Bi Y, Ma X, Zhan F, Wang L, Hu T, Zhou H, Hu Z, Zhou W, Zhao L, Chen J, Meng Y, Wang J, Lin Y, Yuan J, Xie Z, Ma J, Liu WJ, Wang D, Xu W, Holmes EC, Gao GF, Wu G, Chen W, Shi W, Tan W. Genomic characterisation and epidemiology of 2019 novel coronavirus: implications for virus origins and receptor binding. *Lancet* **2020**;395:565–574.

64. Diao B, Wen K, Zhang J, Chen J, Han C, Chen Y, Wang S, Deng G, Zhou H, Wu Y. Accuracy

of a nucleocapsid protein antigen rapid test in the diagnosis of SARS-CoV-2 infection. *Clin Microbiol Infect* **2021**;27:289.e1–289.e4.

65. Wu F, Zhao S, Yu B, Chen YM, Wang W, Song ZG, Hu Y, Tao Z-W, Tian J-H, Pei YY, Yuan ML, Zhang YL, Dai FH, Liu Y, Wang QM, Zheng JJ, Xu L, Holmes EC, Zhang YZ. A new coronavirus associated with human respiratory disease in China. *Nature* **2020**;579:265–269.

66. Deng J, Tian F, Liu C, Liu Y, Zhao S, Fu T, Sun J, Tan W. Rapid one-step detection of viral particles using an aptamer-based thermophoretic assay. *J Am Chem Soc* **2021**;143:7261–7266.

67. Zhang GQ, Gao Z, Zhang J, Ou H, Gao H, Kwok RTK, Ding D, Tang BZ. A wearable AIEgen-based lateral flow test strip for rapid detection of SARS-CoV-2 RBD protein and N protein. *Cell Rep Phys Sci* **2022**;3:100740.

68. Anaissie EJ, Bodey GP, Rinaldi MG. Emerging fungal pathogens. *Eur. J. Clin. Microbiol Infect Dis* **1989**;8:323–330.

69. Gnat S, Łagowski D, Nowakiewicz A, Dyląg M. A global view on fungal infections in humans and animals: opportunistic infections and microsporidioses. *J Appl Microbiol* **2021**;131:2095–2113.

70. Kuper KM, Coyle EA, Wanger A. Antifungal susceptibility testing: A primer for clinicians. *Pharmacotherapy* **2012**;32:1112–1122.

71. Rex John H, Pfaller Michael A, Walsh Thomas J, Chaturvedi V, Espinel-Ingroff A, Ghannoum Mahmoud A, Gosey Linda L, Odds Frank C, Rinaldi Michael G, Sheehan Daniel J, Warnock David W. Antifungal susceptibility testing: Practical aspects and current challenges. *Clin Microbiol Rev* **2001**;14:643–658.

72. Sohnle PG, Hahn BL, Erdmann MD. Effect of fluconazole on viability of candida albicans over extended periods of time. *Antimicrob Agents Chemother* **1996**;40:2622–2625.

73. Chermsirivathana S. A rapid method of staining for fungus and monilial infection. *J Invest Dermatol* **1952**;19:7–8.

74. Webb RJ, Berger L, Skerratt LF, Roberts AA. A rapid and inexpensive viability assay for zoospores and zoosporangia of batrachochytrium dendrobatidis. *J Microbiol Methods* **2019**;165:105688.

75. Giepmans BNG, Adams SR, Ellisman MH, Tsien RY. The Fluorescent toolbox for assessing protein location and function. *Science* **2006**;312:217–224.

76. Hu R, Deng Q, Tang Q, Zhang R, Wang L, Situ B, Gui C, Wang Z, Tang BZ. More is less: Creation of pathogenic microbe-related theranostic oriented AIEgens. *Biomaterials* **2021**;271:120725.

77. Sayed SM, Li XF, Jia H-R, Durrani S, Wu F-G, Lu X. A dibenzothiophene core-based small-molecule AIE probe for wash-free and selective staining of lipid droplets in live mammalian and fungal cells. *Sens Actuators B* **2021**;343:130128.

78. Ge X, Gao M, Situ B, Feng W, He B, He X, Li S, Ou Z, Zhong Y, Lin Y, Ye X, Hu X, Tang BZ, Zheng L. One-step, rapid fluorescence sensing of fungal viability based on a bioprobe with aggregation-induced emission characteristics. *Mater Chem Front* **2020**;4:957–964.

79. Ge X, Gao M, He B, Cao N, Li K, Liu Y, Tang S, Liu K, Zhang J, Hu F, Zheng L, Situ B. Rapid and high-throughput testing of antifungal susceptibility using an AIEgen-based analytical system. *Biomaterials* **2022**;287:121618.

80. Ran B, Wang Z, Cai W, Ran L, Xia W, Liu W, Peng X. Organic photo-antimicrobials: Principles, molecule design, and applications. *J Am Chem Soc* **2021**;143:17891–17909.

81. Nguyen VN, Zhao Z, Tang BZ, Yoon J. Organic photosensitizers for antimicrobial

phototherapy. *Chem Soc Rev* **2022**;51:3324–3340.

82.   Li Y, Zhao Z, Zhang J, Kwok RTK, Xie S, Tang R, Jia Y, Yang J, Wang L, Lam JWY, Zheng W, Jiang X, Tang BZ. A bifunctional aggregation-induced emission luminogen for monitoring and killing of multidrug-resistant bacteria. *Adv Funct Mater* **2023**;33:2213353.

83.   Huang Y, Li D, Wang D, Chen X, Ferreira L, Martins MCL, Wang Y, Jin Q, Wang D, Tang BZ, Ji J. A NIR-II emissive polymer AIEgen for imaging-guided photothermal elimination of bacterial infection. *Biomaterials* **2022**;286:121579.

84.   Kardos N, Demain AL. Penicillin: The medicine with the greatest impact on therapeutic outcomes. *Appl Microbiol Biotechnol* **2011**;92:677–687.

85.   Neu HC. The crisis in antibiotic resistance. *Science* **1992**;257:1064–1073.

86.   Frieri M, Kumar K, Boutin A. Antibiotic resistance. *J Infect Public Health* **2017**;10:369–378.

87.   Stone MRL, Butler MS, Phetsang W, Cooper MA, Blaskovich MAT. Fluorescent antibiotics: New research tools to fight antibiotic resistance. *Trends Biotechnol* **2018**;36:523–536.

88.   Wang B, Wang L, Wu H, Liu X, Zhu J, Hu R, Ding D, Qin A, Tang BZ. The commercial antibiotics with inherent AIE feature: In situ visualization of antibiotic metabolism and specifically differentiation of bacterial species and broad-spectrum therapy. *Bioact Mater* **2023**;23:223–233.

89. Wang B, Wang L, Liu X, Zhu J, Hu R, Qin A, Tang BZ. AIE-active antibiotic photosensitizer with enhanced fluorescence in bacteria infected cells and better therapy effect toward drug-resistant bacteria. *ACS Appl Bio Mater* **2022**;5:4955–4964.

90.   Xie S, Manuguri S, Proietti G, Romson J, Fu Y, Inge AK, Wu B, Zhang Y, Hall D, Ramstrom O, Yan M. Design and synthesis of theranostic antibiotic nanodrugs that display enhanced antibacterial activity and luminescence. *Proc Natl Acad Sci U S A* **2017**;114:8464–8469.

91.   Lee MMS, Yu EY, Chau JHC, Lam JWY, Kwok RTK, Wang D, Tang BZ. Inspiration from nature: BioAIEgens for biomedical and sensing applications. *Biomaterials* **2022**;288:121712.

92.   Lee MMS, Wu Q, Chau JHC, Xu W, Yu EY, Kwok RTK, Lam JWY, Wang D, Tang BZ. Leveraging bacterial survival mechanism for targeting and photodynamic inactivation of bacterial biofilms with red natural AIEgen. *Cell Rep Phys Sci* **2022**;3:100803.

93.   Liang Y, Liang Y, Zhang H, Guo B. Antibacterial biomaterials for skin wound dressing. *Asian J Pharm Sci* **2022**;17:353–384.

94.   Homaeigohar S, Boccaccini AR. Antibacterial biohybrid nanofibers for wound dressings. *Acta Biomater* **2020**;107:25–49.

95.   Dong R, Li Y, Chen M, Xiao P, Wu Y, Zhou K, Zhao Z, Tang BZ. In situ electrospinning of aggregation-induced emission nanofibrous dressing for wound healing. *Small Methods* **2022**;6:e2101247.

96.   Hamblin MR, Hasan T. Photodynamic therapy: A new antimicrobial approach to infectious disease? *Photochem Photobiol Sci* **2004**;3:436–450.

97. Kang M, Zhou C, Wu S, Yu B, Zhang Z, Song N, Lee MMS, Xu W, Xu FJ, Wang D, Wang L, Tang BZ. Evaluation of structure-function relationships of aggregation-induced emission luminogens for simultaneous dual applications of specific discrimination and efficient photodynamic killing of Gram-positive bacteria. *J Am Chem Soc* **2019**;141:16781–16789.

98. Busscher HJ, van der Mei HC, Subbiahdoss G, Jutte PC, van den Dungen JJAM, Zaat SAJ, Schultz MJ, Grainger DW. Biomaterial-associated infection: Locating the finish line in the race for the surface. *Sci Transl Med* **2012**;4:153rv10.

99. He W, Zhang Z, Chen J, Zheng Y, Xie Y, Liu W, Wu J, Mosselhy DA. Evaluation of the anti-

biofilm activities of bacterial cellulose-tannic acid-magnesium chloride composites using an in vitro multispecies biofilm model. *Regener Biomater* **2021**;8:rbab054.

100. Mah T-FC, O'Toole GA. Mechanisms of biofilm resistance to antimicrobial agents. *Trends Microbiol* **2001**;9:34–39.

101. Xu PY, Kankala RK, Li YW, Wang SB, Chen AZ. Synergistic chemo-/photothermal therapy based on supercritical technology-assisted chitosan-indocyanine green/luteolin nanocomposites for wound healing. *Regen Biomater* **2022**;9:rbac072.

102. He W, Wang Z, Bai H, Zhao Z, Kwok RTK, Lam JWY, Tang BZ. Highly efficient photothermal nanoparticles for the rapid eradication of bacterial biofilms. *Nanoscale* **2021**;13:13610–13616.

103. Xu W, Zhang Z, Kang M, Guo H, Li Y, Wen H, Lee MMS, Wang Z, Kwok RTK, Lam JWY, Li K, Xi L, Chen S, Wang D, Tang BZ. Making the best use of excited-state energy: Multimodality theranostic systems based on second near-infrared (NIR-II) aggregation-induced emission luminogens (AIEgens). *ACS Materials Letters* **2020**;2:1033–1040.

104. Zhang Z, Xu W, Kang M, Wen H, Guo H, Zhang P, Xi L, Li K, Wang L, Wang D, Tang BZ. An all-round athlete on the track of phototheranostics: Subtly regulating the balance between radiative and nonradiative decays for multimodal imaging-guided synergistic therapy. *Adv Mater* **2020**;32:e2003210.

105. Li M, Wen H, Li H, Yan ZC, Li Y, Wang L, Wang D, Tang BZ. AIEgen-loaded nanofibrous membrane as photodynamic/photothermal antimicrobial surface for sunlight-triggered bioprotection. *Biomaterials* **2021**;276:121007.

106. Wu J, Zhang W-S, Zhao J, Zhou H-Y. Review of clinical and basic approaches of fungal keratitis. *Int J Ophthalmol* **2016**;9:1676–1683.

107. Hay RJ. Fungal infections. *Clin Dermatol* **2006**;24:201–212.

108. Bai H, He W, Chau JHC, Zheng Z, Kwok RTK, Lam JWY, Tang BZ. AIEgens for microbial detection and antimicrobial therapy. *Biomaterials* **2021**;268:120598.

109. Chatre L, Ricchetti M. Are mitochondria the Achilles' heel of the Kingdom Fungi? *Curr Opin Microbiol* **2014**;20:49–54.

110. McLellan CA, Vincent BM, Solis NV, Lancaster AK, Sullivan LB, Hartland CL, Youngsaye W, Filler SG, Whitesell L, Lindquist S. Inhibiting mitochondrial phosphate transport as an unexploited antifungal strategy. *Nat Chem Biol* **2018**;14:135–141.

111. Zhou C, Peng C, Shi C, Jiang M, Chau JHC, Liu Z, Bai H, Kwok RTK, Lam JWY, Shi Y, Tang BZ. Mitochondria-specific aggregation-induced emission luminogens for selective photodynamic killing of fungi and efficacious treatment of keratitis. *ACS Nano* **2021**;15:12129–12139.

112. Li H, Zhang L, Han J, Kim D, Kim H, Ha J, Wang J, Yoon J. Molecular structural evolution of near-infrared cationic aggregation-induced emission luminogens: preclinical antimicrobial pathogens activities and tissues regeneration. *CCS Chem* **2022**;4:487–500.

113. Leung NHL, Chu DKW, Shiu EYC, Chan KH, McDevitt JJ, Hau BJP, Yen HL, Li Y, Ip DKM, Peiris JSM, Seto WH, Leung GM, Milton DK, Cowling BJ. Respiratory virus shedding in exhaled breath and efficacy of face masks. *Nat Med* **2020**;26:676–680.

114. Liao L, Xiao W, Zhao M, Yu X, Wang H, Wang Q, Chu S, Cui Y. Can N95 respirators be reused after disinfection? How many times? *ACS Nano* **2020**;14:6348–6356.

115. Ahmed W, Angel N, Edson J, Bibby K, Bivins A, O'Brien JW, Choi PM, Kitajima M, Simpson SL, Li J, Tscharke B, Verhagen R, Smith WJM, Zaugg J, Dierens L, Hugenholtz P, Thomas KV, Mueller JF. First confirmed detection of SARS-CoV-2 in untreated wastewater in Australia: A proof

of concept for the wastewater surveillance of COVID-19 in the community. *Sci Total Environ* **2020**;728:138764.

116. Li B, Wang D, Lee MMS, Wang W, Tan Q, Zhao Z, Tang BZ, Huang X. Fabrics attached with highly efficient aggregation-induced emission photosensitizer: Toward self-antiviral personal protective equipment. *ACS Nano* **2021**;15:13857–13870.

117. Zou S, Wang B, Wang C, Wang Q, Zhang L. Cell membrane-coated nanoparticles: research advances. *Nanomedicine* **2020**;15:625–641.

118. Li B, Wang W, Song W, Zhao Z, Tan Q, Zhao Z, Tang L, Zhu T, Yin J, Bai J, Dong X, Tan S, Hu Q, Tang BZ, Huang X. Antiviral and anti-inflammatory treatment with multifunctional alveolar macrophage-like nanoparticles in a surrogate mouse model of COVID-19. *Adv Sci* **2021**;8:2003556.

119. Wu MY, Gu M, Leung JK, Li X, Yuan Y, Shen C, Wang L, Zhao E, Chen S. A Membrane-targeting photosensitizer with aggregation-induced emission characteristics for highly efficient photodynamic combat of human coronaviruses. *Small* **2021**;17:e2101770.

120. Lin L, Du Y, Song J, Wang W, Yang C. Imaging commensal microbiota and pathogenic bacteria in the gut. *Acc Chem Res* **2021**;54:2076–2087.

121. Chong CR, Sullivan DJ. New uses for old drugs. *Nature* **2007**;448:645–646.

122. Feng Z, Bai S, Qi J, Sun C, Zhang Y, Yu X, Ni H, Wu D, Fan X, Xue D, Liu S, Chen M, Gong J, Wei P, He M, Lam JWY, Li X, Tang BZ, Gao L, Qian J. Biologically excretable aggregation-induced emission dots for visualizing through the marmosets intravitally: Horizons in future clinical nanomedicine. *Adv Mater* **2021**;33:2008123.